Therapeutics, Targets, and Chemical Biology

Cancer Research

R428, a Selective Small Molecule Inhibitor of Axl Kinase, Blocks Tumor Spread and Prolongs Survival in Models of Metastatic Breast Cancer

Sacha J. Holland[1], Alison Pan[1], Christian Franci[1], Yuanming Hu[1], Betty Chang[1], Weiqun Li[1], Matt Duan[1], Allan Torneros[1], Jiaxin Yu[1], Thilo J. Heckrodt[1], Jing Zhang[1], Pingyu Ding[1], Ayodele Apatira[1], Joanne Chua[2], Ralf Brandt[2], Polly Pine[1], Dane Goff[1], Rajinder Singh[1], Donald G. Payan[1], and Yasumichi Hitoshi[1]

Abstract

Accumulating evidence suggests important roles for the receptor tyrosine kinase Axl in cancer progression, invasion, metastasis, drug resistance, and patient mortality, highlighting Axl as an attractive target for therapeutic development. We have generated and characterized a potent and selective small-molecule inhibitor, R428, that blocks the catalytic and procancerous activities of Axl. R428 inhibits Axl with low nanomolar activity and blocked Axl-dependent events, including Akt phosphorylation, breast cancer cell invasion, and proinflammatory cytokine production. Pharmacologic investigations revealed favorable exposure after oral administration such that R428-treated tumors displayed a dose-dependent reduction in expression of the cytokine granulocyte macrophage colony-stimulating factor and the epithelial-mesenchymal transition transcriptional regulator Snail. In support of an earlier study, R428 inhibited angiogenesis in corneal micropocket and tumor models. R428 administration reduced metastatic burden and extended survival in MDA-MB-231 intracardiac and 4T1 orthotopic (median survival, >80 days compared with 52 days; $P < 0.05$) mouse models of breast cancer metastasis. Additionally, R428 synergized with cisplatin to enhance suppression of liver micrometastasis. Our results show that Axl signaling regulates breast cancer metastasis at multiple levels in tumor cells and tumor stromal cells and that selective Axl blockade confers therapeutic value in prolonging survival of animals bearing metastatic tumors. *Cancer Res; 70(4); 1544–54. ©2010 AACR.*

Introduction

Axl is a member of the TAM (Tyro3, Axl, Mer) receptor tyrosine kinase (RTK) family and was originally identified as a transforming gene expressed in cells from patients with chronic myelogenous leukemia (1) or chronic myeloproliferative disorder (2). Axl activation occurs by binding of its cognate protein ligand, growth arrest specific 6 (Gas6), homotypic dimerization through its extracellular domain or cross-talk via the interleukin (IL)-15 receptor (3, 4) or HER2 (5). Axl signaling stimulates cellular responses, including activation of phosphoinositide 3-kinase–Akt, extracellular signal-regulated kinase (ERK) and p38 mitogen-activated protein kinase cascades, the NF-κB pathway, and signal transducer and activator of transcription (STAT) signaling (3). Moreover, many biological consequences of Axl signaling, including invasion, migration, survival signaling, angiogenesis, resistance to chemotherapeutic and targeted drugs, cell transformation, and proliferation, represent undesirable traits associated with cancer (4).

We previously uncovered the association between Axl and regulation of cell migration using a functional genetic screen designed to identify regulators of haptotaxis in primary human endothelial cells (6). Subsequent studies from other groups strongly support a central role for Axl in control of tumor cell migration and invasion (7–12). Importantly, Axl-dependent changes in invasive cell behavior are also observed on manipulation of Axl signaling in gliomas *in vivo* (7).

High Axl expression is observed in many human tumors and is associated with tumor progression in cancer patients. Axl expression in primary lung and pancreatic adenocarcinomas is correlated with lymph node status (8, 10) and/or disseminated disease (10). In glioblastoma multiforme (GBM), Axl expression is associated with an actively migrating cell population that predicts aggressive behavior (13). Importantly, patients whose primary pancreatic, esophageal, lung, breast, renal cell carcinoma, GBM, or acute myeloid leukemia expressed high levels of Axl had shorter progression-free and overall survival (8, 10, 13–16).[3] These data suggest that Axl

Authors' Affiliations: [1]Rigel, Inc., South San Francisco, California and [2]*vivo*Pharm Pty. Ltd., Adelaide, South Australia, Australia

Note: Supplementary data for this article are available at Cancer Research Online (http://cancerres.aacrjournals.org/).

Corresponding Author: Sacha J. Holland, Rigel, Inc., 1180 Veteran's Boulevard, South San Francisco, CA 94112. Phone: 650-624-1283; Fax: 650-624-1101; E-mail: sholland@rigel.com.

doi: 10.1158/0008-5472.CAN-09-2997

[3] Alvarez et al., in preparation.

expression confers aggressive tumor behavior, leading to tumor dissemination and mortality from metastasis.

Axl has been established as a strong candidate drug target for therapeutic inhibition of cancer invasion and dissemination. As metastatic disease is the most frequent cause of cancer patient mortality (17), therapeutics specifically aimed at inhibiting metastatic dissemination and colonization would be important additions to the arsenal of drugs in clinical use. We therefore identified an orally bioavailable, potent, and selective small-molecule inhibitor of Axl kinase, R428. R428 retards cancer cell migration and invasion *in vitro*, is well tolerated *in vivo*, and blocks metastasis development in two independent mouse models of breast cancer dissemination. Moreover, R428 synergizes with the cytotoxic drug cisplatin to block liver micrometastases. Importantly, R428 extends survival of mice orthotopically implanted with 4T1 breast tumors. These data suggest that blockade of Axl signaling in Axl-expressing human tumors could lead to reduced tumor metastasis and improved patient survival.

Materials and Methods

Reagents

Antibody suppliers were as follows: anti-Axl, R&D Systems, Inc. and Santa Cruz Biotechnology, Inc.; anti-phosphotyrosine, Santa Cruz Biotechnology; anti–phospho-Akt (Ser^{473}) and anti-mouse Snail, Cell Signaling Technology; and anti-actin, Cytoskeleton, Inc. Phospho-Axl antibodies were raised against the phospho-peptide PDEIL(pY_{821}) VNMDE (Quality Controlled Biochemicals). Gas6 and Axl-Fc were from R&D Systems. 4T1, HeLa, and K562 cell lines were obtained from the American Type Culture Collection. MDA-MB-231-luc-D3H2LN cells (18) were from Xenogen/Caliper.

R428

R428 (19) was discovered and synthesized at Rigel, Inc. High-throughput screening was performed using an *in vitro* Axl kinase assay. On-target SAR was tracked using the HeLa cell-based assay and the Axl biochemical assay (see below). R428 was formulated for *in vivo* studies in 0.5% hydroxypropylmethylcellulose + 0.1% Tween 80.

Cell Culture

MDA-MB-231 cells were grown as in ref. 6. 4T1 cells were maintained in RPMI 1640 (Mediatech)/10% FCS (S.A.F.C. Bioscience) for *in vitro* experiments and RPMI 1640/10% FCS (Invitrogen Australia)/50 IU/mL penicillin/streptomycin (Sigma-Aldrich) for metastasis models. For Western blot and cytokine analysis, 2×10^5 cells per well were plated in six-well plates and starved for 24 h in medium/0.5% serum ± 500 ng/mL Axl-Fc. Medium was replaced with growth medium/0.5% serum before R428 preincubation and stimulation using antibody cross-linking, huGas6 (2 μg/mL) or muGas6 (5 μg/mL).

Cytokine Expression

4T1 cells were starved in medium/0.5% FCS overnight. Cytokines in conditioned medium and tumor lysate were analyzed in triplicate using a Milliplex kit (Millipore). Plates were read on a Luminex 100 system.

Tumor Lysates

Frozen tumor tissue was crushed in a precooled BioPulverizer (Biospec) and lysed in phospholipase C lysis buffer (6) with homogenization. Protein concentration was determined using a bicinchoninic acid assay (Thermo Scientific). Snail expression was quantified using Alpha Ease FC (Alpha Innotech).

Axl Cell-Based Assay

HeLa cells were seeded in starvation medium in 96-well plates. Twenty-four hours later, cells were preincubated for 1 h with diluted R428 before stimulation with preclustered anti-Axl antibody. Cells were fixed, blocked, and stained with anti–phospho-Akt (Ser^{473}) followed by goat anti-rabbit horseradish peroxidase (Jackson ImmunoResearch) before developing using SuperSignal ELISA Pico chemiluminescent substrate (Thermo Scientific). See also Supplementary Materials and Methods.

In vitro Kinase Assays

A five-point R428 dose titration was performed in radiometric *in vitro* kinase assays on 133 kinases at the K_m^{ATP} for each kinase (Millipore). Axl, Mer, and Tyro3 (Carna Biosciences) assays were also performed using a fluorescence polarization protocol (20). HER2 activity was determined by Z'-LYTE assay (Invitrogen).

Invasion Assays

MDA-MB-231 or 4T1 cells (1×10^5) were allowed to migrate through Matrigel (Millipore) toward 20% FCS in an 8-μm pore 24-well Transwell plate (BD Bio-sciences) at 37°C for 16 to 24 h. Noninvaded cells and Matrigel were removed by swabbing. Invaded cells were fixed in 4% formaldehyde, stained with 1% crystal violet, and quantified as for Axl cell-based assay. Cells were preincubated with R428 for 3 h. R428 was added to both upper and lower Transwell chambers.

MDA-MB-231-luc-D3H2LN Intracardiac Model (Molecular Imaging Research)

Seven- to 8-wk-old female NCr *nu/nu* mice (Taconic) were injected intracardially with bioluminescent MDA-MB-231-luc-D3H2LN cell suspension (18). Oral dosing with R428 (125 mg/kg) or vehicle twice daily began 2 h before cell implantation and continued to day 21 ($n = 20$). Metastatic burden was quantified by *in vivo* bioluminescence imaging on day 22 and analyzed using the Wilcoxon rank sum test (Microsoft Excel, Microsoft).

4T1 Orthotopic Model (*vivo*Pharm Pty. Ltd.)

Female BALB/c mice were inoculated in the mammary fat pad with 0.5×10^6 4T1 cells. Forty-eight hours after inoculation, mice were randomized into treatment groups ($n = 10$). Oral dosing with R428 (7–75 mg/kg twice daily) or vehicle continued until days 19 to 21. Cisplatin (1.2 or 4 mg/kg; Mayne Pharma) was administered i.v. once weekly. Body weight and tumor size were measured thrice per week. Lungs

were exposed postmortem. Total number and size of surface lung macrometastases were measured (small, <2 mm; medium, ≥2 mm and <3 mm; large, ≥3 mm). Half of each primary tumor was snap frozen in liquid nitrogen. The other half, and the livers, were fixed in paraformaldehyde/lysine/periodate solution (21), paraffin embedded, and sectioned (5 μm thick). Two H&E-stained liver sections per animal were examined microscopically for micrometastases in three view fields. Synergism was determined using Clark's synergy calculation (22).

Mastectomy study (n = 12 per group). On day 5 after inoculation, the primary tumor and mammary fat pad were excised. No treatments were administered on the day of mastectomy or the following morning. Individual animals were culled due to adverse clinical signs and the study was terminated on day 81. Tissue sections from multiple organs were analyzed by a pathologist.

Statistical Analysis

Unless otherwise noted, the *t* test was used. Statistics were performed using Prism v4.0c (GraphPad Prism) and SigmaStat 3.0 (SPSS Australasia). *, $P < 0.05$; **, $P < 0.01$; ***, $P < 0.001$. Comparisons that did not reach statistical significance were not noted.

Results

R428 is a selective small-molecule inhibitor of Axl kinase. A high-throughput screen, followed by structure-activity relationship (SAR) modifications, was performed to specifically identify potent small-molecule inhibitors of Axl kinase activity and refine selectivity against other cellular targets. R428 (1-(6,7-dihydro-5*H*-benzo[6,7]cyclohepta[1,2-*c*]pyridazin-3-yl)-*N*3-((7-pyrrolidin-1-yl)-6,7,8,9-tetrahydro-5H-benzo[7]annulene-2-yl)-1*H*-1,2,4-triazole-3,5-diamine) (Fig. 1A; ref. 19), the lead compound from this SAR, exhibited potent activity (EC_{50}/IC_{50}, 14 nmol/L) in both *in vitro* biochemical kinase assays using recombinant Axl protein (Fig. 1B) and a cell-based assay reflecting Axl signaling in HeLa cells that uses downstream phosphorylation of Akt on Ser^{473} as the readout (Fig. 1C, i and ii). Moreover, R428 potently blocked autophosphorylation on a COOH-terminal multiple docking site, Tyr^{821} (23), stimulated by either antibody-mediated cross-linking or Gas6 (Fig. 1C, iii). Inhibition of Axl signaling was comparable in different Axl-expressing cells, including human MDA-MB-231 and murine 4T1 breast cancer cells and human umbilical vein endothelial cells (Supplementary Fig. S1A-C).

R428 activity was evaluated in a broad panel of 133 tyrosine and serine/threonine kinases using *in vitro* enzymatic assays (Table 1). R428 activity was limited to the tyrosine kinase subfamily. Of the 133 kinases, Axl was most potently inhibited by R428. With the exception of Tie-2, Ftl-1, Flt-3, Ret, and Abl, kinase inhibition by R428 was at least 10 times lower than observed for Axl. In contrast, R428 exhibited >100-fold selectivity for Axl versus Abl and 50- and >100-fold selectivity over TAM family kinases Mer and Tyro3, respectively, in cells (Table 1). R428 was >100-fold selective for Axl over insulin receptor, epidermal growth factor receptor (EGFR), HER2, and platelet-derived growth factor receptor β (PDGFRβ) and kinases of other subfamilies. Moreover, R428 had minimal off-target antiproliferative or cytotoxic activity in two-dimensional assays in several cell types (Supplementary Table S1). Although Axl inhibition has been observed in some multitargeted tyrosine kinase inhibitors (Supplementary Table S2; refs. 12, 24, 25), R428 is, to the best of our knowledge, unique in its nanomolar on-target activity and restricted selectivity profile.

***R428 inhibits invasion of breast cancer cells* in vitro.** To validate cell lines for use in *in vivo* efficacy models, we confirmed previous observations that inhibition of Axl expression blocks breast cancer cell invasion (Supplementary Fig. S1D and E). Correspondingly, R428 dose dependently suppressed invasion of both human MDA-MB-231 and murine 4T1 breast cancer cell lines (Fig. 1D). R428 did not strongly inhibit proliferation of either cell line in two-dimensional assays (Supplementary Fig. S1F and H), correlating with the lack of effect of Axl knockdown (6). However, R428 did modestly reduce 4T1 survival in low serum conditions (Supplementary Fig. S1I).

***R428 exhibits high exposure* in vivo.** R428 was very stable (half-life, ≥60 minutes) in hepatic microsome preparations from several species, indicating a low susceptibility to liver metabolism (Supplementary Fig. S2A).

A single administration of R428, delivered to female BALB/c mice by oral gavage, resulted in high plasma exposures (C_{max} of approximately 2.6 and 6.8 μmol/L with doses of 25 and 75 mg/kg, respectively) with linear dose proportionality up to 100 mg/kg (Supplementary Fig. S2B). R428 exhibited a long plasma half-life (4 hours at 25 mg/kg; 13 hours at 75 mg/kg) and distributed effectively to tissues (Supplementary Fig. S2A). Predose levels of approximately 2.4, 6.8, and 9.0 μmol/L were observed after prolonged twice-daily R428 dosing at 25, 50, and 100 mg/kg, respectively, showing that high steady-state plasma drug concentrations were achievable (Supplementary Fig. S2C). R428 blocked Gas6-induced Axl phosphorylation in mouse blood with EC_{50} of 0.1 to 1 μmol/L (Supplementary Fig. S2D), indicating that prolonged dosing with only 25 mg/kg R428 twice daily generates a steady-state R428 concentration sufficient to block Axl signaling in the circulation.

R428 suppresses breast cancer metastasis in two independent* in vivo *models. R428 efficacy was examined in two *in vivo* models of invasion and metastasis. Initially, we used a model in which highly metastatic, bioluminescent MDA-MB-231-luc-D3H2LN cells are injected intracardially, producing widespread arterial dissemination, allowing tumor seeding in soft tissue and bone (18). R428 treatment was initiated 2 hours before cell injection in a prevention protocol (Fig. 2A). Metastasis development was detected 22 days later by bioluminescent imaging. R428 was well tolerated and no weight loss was observed during treatment (Fig. 2B). R428 treatment significantly blocked development of soft tissue MDA-MB-231-luc-D3H2LN metastases (Fig. 2C). As 100% metastasis incidence was observed in R428-treated groups, treatment may have delayed metastasis or inhibited the growth of micrometastases. A role for Axl in growth in a three-dimensional rather than two-dimensional environment

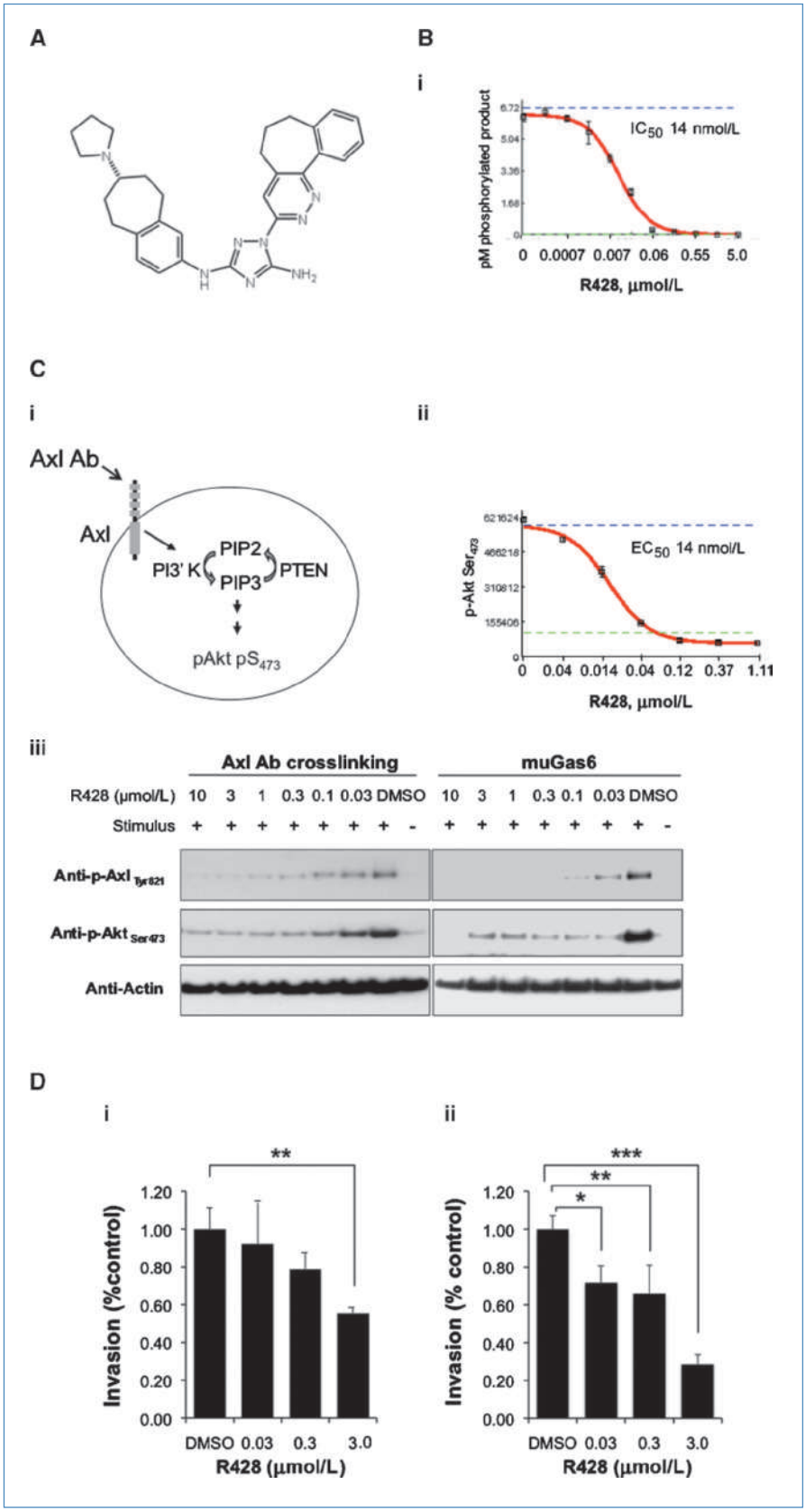

Figure 1. A, chemical structure of R428. B, dose-dependent activity of R428 in a fluorescence polarization–based *in vitro* kinase assay using recombinant Axl protein. Top dashed line, DMSO control; bottom dashed line, reaction lacking substrate. C, phosphorylation of Akt (Ser^{473}) and Axl (Tyr^{821}) is inhibited by R428 in cells. i, schematic of Axl cell-based activity assay. HeLa cells were stimulated using Axl antibody-mediated cross-linking. Phosphorylation of Akt on Ser^{473} was used as surrogate readout for Axl activity. ii, HeLa cells were preincubated with R428 1 h before stimulation for 5 min. Fixed cells were stained with anti–phospho-Akt (Ser^{473}). Top dashed line, stimulated, DMSO control; bottom dashed line, unstimulated, DMSO control. iii, HeLa cells were preincubated with R428 and stimulated with antibody-mediated cross-linking or muGas6. Immunoblots of total cell lysates were probed with anti–phospho-Axl (Tyr^{821}), anti–phospho-Akt (Ser^{473}), or anti-actin. D, R428 reduces invasion of MDA-MB-231 (i) and 4T1 (ii) cells. Cells were starved overnight in medium containing 0.5% serum and 0.5 μg/mL Axl-Fc. After 3-h R428 preincubation, invasion through Matrigel in a Boyden chamber toward 20% serum was carried out in the presence of R428 for 16 to 24 h. MDA-MB-231, $n = 3$; 4T1, $n = 4$. *, $P < 0.05$; **, $P < 0.01$; ***, $P < 0.001$.

Table 1. Selectivity of R428 in cell-based and biochemical assays

Kinase	Kinase family and group	Fold over Axl	
		Biochemical	Cell-based
Mer	TK	16	50
Tyro3	TK	14	>100
Tie-2	TK	3	ND
Flt-1, Flt-4	TK	8.0, 5.5	ND
Insulin receptor	TK	>50	>100
VEGFR2	TK	34	33
EGFR, HER2	TK	>100	>100, ND
PDGFRβ	TK	>100	>100
Ret	TK	9	ND
Met	TK	>100	ND
Abl	TK	9.3	>100
c-Src, JAK3	TK	>100	ND, >50
c-raf	TKL	>100	ND
MEK1, Pak2	STE	>100	ND
CK1γ2, CK2	CK1	>100	ND
p70S6K, PKCγ, PKCε	AGC	>100	ND
AMPK, CAMKIIβ, MLCK	CAMK	>100	ND
CDK2, ERK1	CMGC	>100	ND

NOTE: Biochemical: fold difference between R428 IC_{50} in off-target versus Axl biochemical assays. Cell-based: fold difference between R428 EC_{50} in off-target versus Axl cell-based assays. Phosphorylation-based signaling assays were used except for Abl and JAK3 (proliferation readout).

Abbreviation: ND, not determined; TK, tyrosine kinase; TKL, tyrosine kinase-like; STE, homologues of yeast Sterile 7, Sterile 11, Sterile 20 kinases; CK1, Casein kinase 1; AGC, containing PKA, PKG, PKC families; CAMK, calcium/calmodulin-dependent protein kinases; CMGC, containing CDK, MAPK, GSK3, CLK families.

is supported by our previously published MDA-MB-231 xenograft study (6).

In a separate study arm, MDA-MB-231-luc-D3H2LN metastases were allowed to develop for 14 days before initiation of R428 treatment. A trend toward delayed metastasis growth and concomitant prolonged survival was observed in R428-treated animals using this protocol (Supplementary Fig. S3). Together, these data indicate that R428 suppresses metastasis development in the experimental MDA-MB-231-luc-D3H2LN model.

Next, we tested R428 efficacy in the orthotopic 4T1 model (Fig. 3A). 4T1 cells metastasize aggressively to lung and liver. This model exhibits a profound tumor-derived cytokine-induced host "leukemoid" response, including significant $CD11b^{+}Gr\text{-}1^{+}$ cell expansion, and reflects all steps of breast cancer metastasis development in an immunocompetent host (26–29).

As expected, R428 had no effect on body weight (Fig. 3B), implantation rate, or growth of the primary tumor (Supplementary Fig. S4A and B). However, R428 treatment reduced lung metastasis. R428 (7 mg/kg twice daily) significantly suppressed both total metastatic burden and the number of larger metastases (medium + large metastases, ≥2 mm diameter; Fig. 3C).

Macroscopic 4T1 lung metastases develop rapidly, whereas the liver is seeded later and presents with micrometastases at 3 weeks (26). R428 treatment potently blocked liver micrometastases (Fig. 3D). Immunostaining with mammary-specific markers mammaglobin (30) and cytokeratin 5 (31) confirmed tumor cell presence in the liver lesions (Supplementary Fig. S4C; Fig. 3D, iii).

Taken together, these data indicate that Axl kinase inhibition by R428 suppresses metastatic seeding from an orthotopic location in an immunocompetent host and may also reduce growth and/or establishment of cancer cells at the metastatic location.

***R428 suppresses angiogenesis* in vivo.** We have previously shown that Axl regulates endothelial migration and angiogenesis (6). Angiogenesis is required for metastasis, both to facilitate escape of cells from the primary tumor and to support growth of nascent metastases. R428 suppressed both tumor angiogenesis and vascular endothelial growth factor (VEGF)–induced corneal neovascularization *in vivo* (Supplementary Fig. S5). Suppression of angiogenesis by R428, therefore, likely contributes to inhibition of metastasis growth.

R428 modulates expression of surrogate markers in tumor tissue. Expression of surrogate markers for Axl activity was analyzed in R428-treated tumor tissue. Axl stimulates phosphorylation of Akt and ERK in culture (3, 4). However, these effectors are targets of multiple upstream inputs *in vivo* and can therefore be challenging to use as surrogate markers. Axl knockdown in pancreatic cancer cells leads to reduced

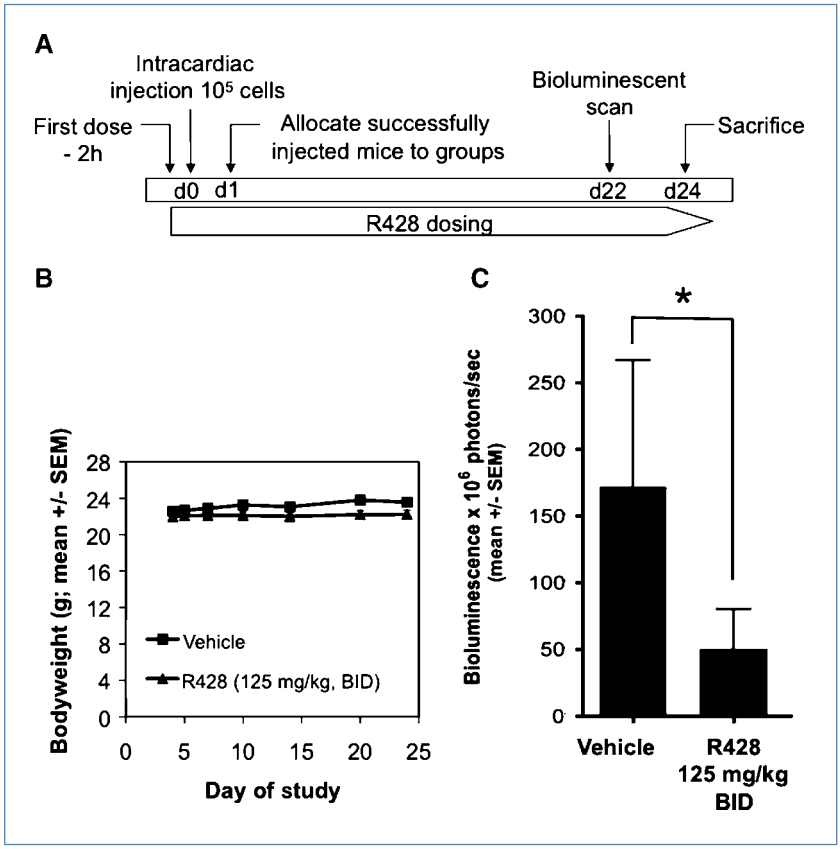

Figure 2. A, experimental protocol for MDA-MB-231-luc-D3H2LN metastasis prevention study. Female nude mice were injected intracardially with 10^5 MDA-MB-231-luc-D3H2LN cells. Twice-daily (BID) treatment with vehicle or R428 at 125 mg/kg was initiated 2 h before cell inoculation and continued for 24 d. A bioluminescent scan was performed at day 22 to determine metastatic burden. B, mean body weight of animals on study. C, R428 significantly reduces total metastatic burden determined by whole-animal bioluminescent scanning. $n = 20$. *, $P < 0.05$ versus vehicle control, Wilcoxon rank sum test.

expression of the epithelial-mesenchymal transition (EMT) regulator Snail (8, 32). We confirmed that Axl regulates Snail expression in cultured 4T1 cells (Fig. 4A, i). Moreover, a dose-dependent trend in reduced Snail expression was observed in lysates from R428-treated primary tumors (Fig. 4A, ii and iii).

Expression of granulocyte macrophage colony-stimulating factor (GM-CSF; Fig. 4B, i) IL-1β, IL-6, and macrophage inflammatory protein-1α (Supplementary Fig. S4D) was also reduced in a dose-dependent manner in primary tumor lysates from R428-treated animals. GM-CSF secretion was Axl dependent in cultured 4T1 cells (Fig. 4B, ii). R428 modulation of GM-CSF expression *in vivo* therefore likely resulted from Axl inhibition in the tumor cell compartment.

These data indicate that R428 levels in tumor tissue are sufficient to affect gene expression and tumor biology downstream of Axl signaling.

R428 extends survival of BALB/c mice inoculated with syngeneic 4T1 breast cancer cells. An inhibitor of metastasis would likely be used clinically in an adjuvant setting (16). We therefore tested R428 in a 4T1 mastectomy protocol. Primary tumor excision 5 days after inoculation allowed mice to live past day 19 (Fig. 5A). Mortality after day 28 is thought to be primarily due to lung metastatic burden.[4]

[4] R. Brandt, unpublished data.

R428-treated animals tended to exhibit fewer total lung metastases than control animals and displayed a propensity toward reduced incidence of lung metastasis (Fig. 5B and C). On histologic examination, metastases were observed in multiple organs of vehicle animals, whereas no metastases were observed in R428-treated mice. Moreover, R428 seemed to reduce the leukemoid reaction/extramedullary hematopoiesis associated with 4T1 tumor physiology (data not shown; refs. 27, 28).

Metastasis-related mortality began in vehicle-treated mice at day 30, and all but one control animal was dead by study termination on day 80 (Fig. 5D, i). R428 treatment significantly prolonged survival, reflecting the observed decreased lung metastasis. Median survival was extended from 52 days in vehicle-treated animals to >80 days in mice treated with 7 mg/kg R428. Although survival of mice treated with R428 (25 mg/kg twice daily) seemed shorter than for the lower dose, there was no significant difference in survival between 25 and 7 mg/kg R428 twice daily–treated groups.

R428 safety was evaluated after long-term dosing in this study as well as in a 14-day tolerability study. R428 was well tolerated at all doses. No significant compound-related weight loss (Fig. 5D, ii), mortality, adverse clinical signs, or organ weight changes were noted.

These data show that R428 can prolong survival in an adjuvant model of breast cancer metastasis, likely due to reduced metastatic burden. Moreover, R428 is well-tolerated even after prolonged dosing.

R428 synergizes with cisplatin to block liver micrometastases. In the clinic, novel cancer therapeutics are usually combined with standard-of-care cytotoxic agents. We therefore tested R428 efficacy in combination with a suboptimal dose (1.2 mg/kg weekly) of cisplatin. Treatment with either 7 or 21 mg/kg R428 twice daily in addition to cisplatin synergistically blocked liver micrometastasis compared with either agent alone (Supplementary Table S3; ref. 22). Moreover, a propensity toward further suppression of larger lung metastases was observed comparing combination treatment with cisplatin alone (Supplementary Fig. S6).

Discussion

In this study, we describe the first potent and selective, targeted Axl inhibitor, R428. R428 blocks Axl signaling and cancer cell invasion *in vitro*. Moreover, inhibition of Axl activity *in vivo* using R428 blocks breast cancer metastasis and prolongs survival.

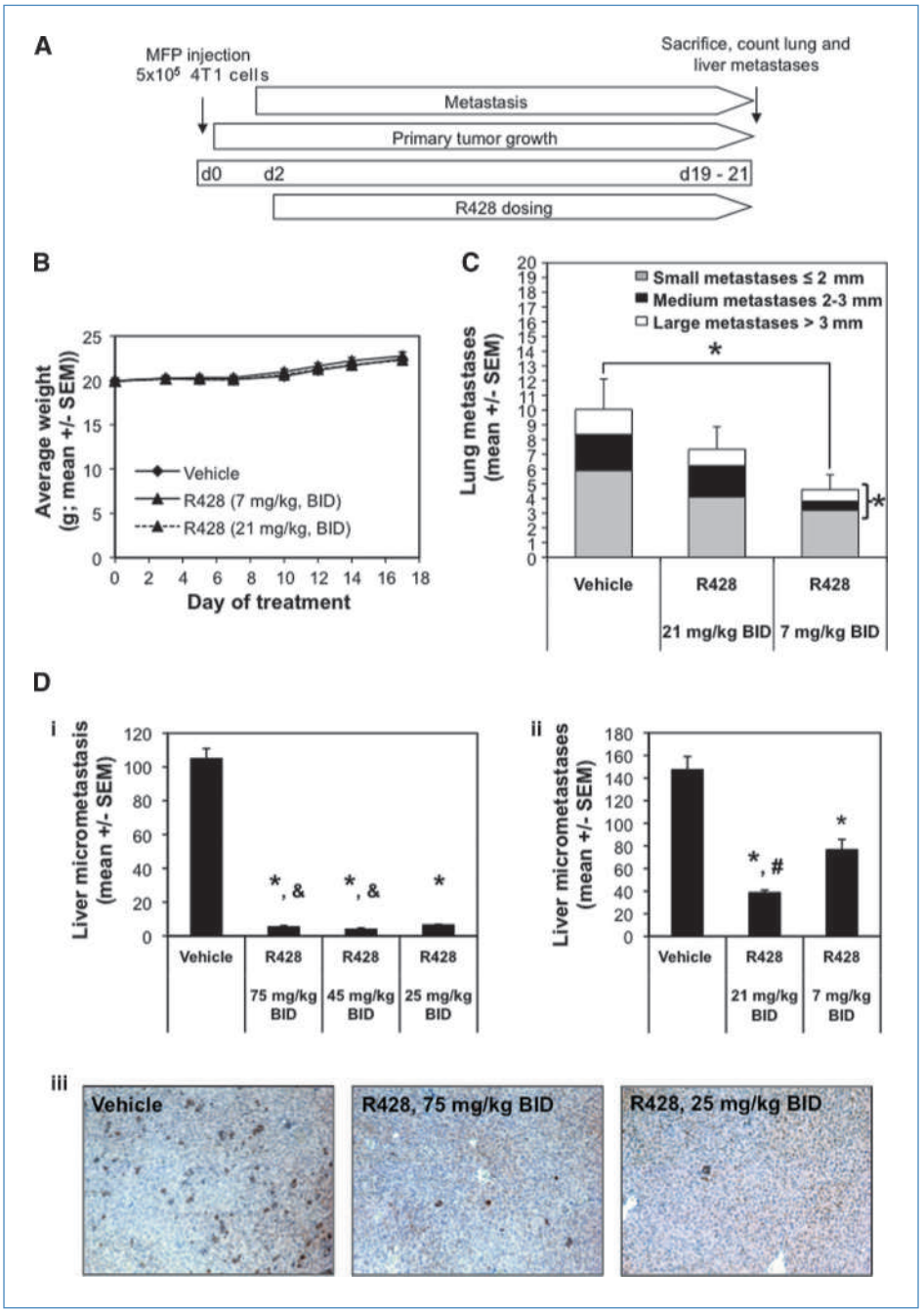

Figure 3. A, experimental protocol for 4T1 orthotopic metastasis study. Female BALB/c mice were injected in the mammary fat pad with 5×10^5 4T1 cells. Treatment with vehicle and R428 twice daily (BID) at 7 and 21 mg/kg (B, C, and Dii) or at 25, 45, and 75 mg/kg (D, i and iii) was initiated on day 2 and continued until termination on day 19 (B, C, and Dii) or day 21 (D, i and iii). B, mean body weight of animals on study. C, R428 treatment reduces 4T1 lung metastasis. Lung metastases were counted at study termination and categorized as small (≤2 mm; gray fill), medium (2–3 mm; black fill), and large (≥3 mm; white fill). SEMs are for mean total metastases. *, $P < 0.05$, total and medium + large metastases (>2 mm) versus vehicle control, *t* test. D, R428 treatment reduces 4T1 liver micrometastases. Livers were sectioned and stained with H&E. H&E-stained colonies were counted in three fields each from two sections per mouse. i and ii, R428 dose response was determined in two separate studies. *, $P < 0.05$ versus vehicle control; &, $P < 0.05$ versus R428 at 25 mg/kg twice daily; #, $P < 0.05$ versus R428 at 7 mg/kg twice daily, Mann-Whitney test. iii, liver sections from study D (i) were stained with anti-mammaglobin to visualize tumor cells. R428 treatment reduces the number of anti-mammaglobin staining liver micrometastases. Magnification, ×10.

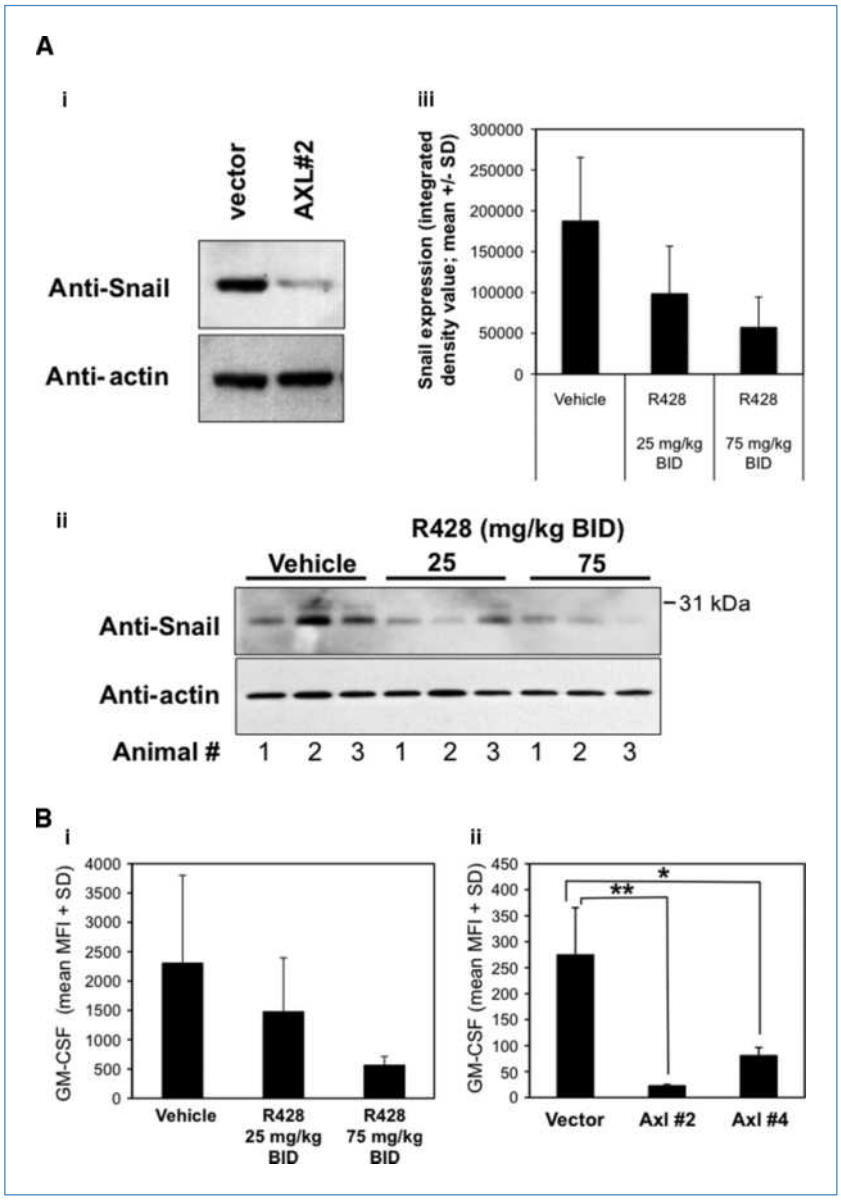

Figure 4. R428 modulates expression of Snail and GM-CSF in 4T1 primary tumors. 4T1 cell populations infected with Axl short hairpin RNAs [Supplementary Fig. S1E; A (i) and B (ii)] or tumors from the study in Fig. 3D, i [A (ii and iii) and B (i)] were lysed. A, i and ii, Western blot with anti-mouse Snail or anti-actin antibodies. iii, quantification of Snail expression in ii. Three mice were analyzed per group. B, GM-CSF expression in tumor lysates (i) or conditioned supernatant (ii) from Axl short hairpin RNA knockdown cell populations was analyzed by Luminex. MFI, median fluorescence intensity; BID, twice daily.

RTKs have been extensively validated as targets for cancer therapeutics (33). Focused cancer drugs that inhibit HER2, VEGF receptor 2 (VEGFR2), and c-Kit have achieved success in improving patient survival in several solid tumor types. Although Axl represents a lesser-studied RTK, persuasive evidence exists for a causative role in cancer progression and spread. First, the cellular outcomes of Axl activation (invasion, migration, survival signaling, angiogenesis, cell transformation, and proliferation) are processes associated with tumorigenesis (4). Second, cells engineered to overexpress Axl acquire a more invasive phenotype both *in vitro* and *in vivo*. Blocking Axl expression or signaling (by expression of dominant-negative Axl or function-blocking antibody) inhibits expression of EMT regulators and cell invasiveness (7–12). Third, Axl upregulation allows cancer cells to acquire resistance to targeted therapeutics (e.g., imatinib and lapatinib) and chemotherapeutics, including doxorubicin, cisplatin, and etoposide (24, 34–36). Fourth, Axl and Gas6 are upregulated by acidosis (37), which occurs as a consequence of hypoxia and correlates with an aggressive and invasive tumor response. Finally, high Axl expression correlates clinically with cancer spread and poor patient prognosis in several cancer types (8, 10, 13–16).[3] Upregulation of Axl signaling may, therefore, be a widespread mechanism by which tumor cells undergo progression and activate invasive behavior. Thus, there is a strong rationale for developing Axl inhibitors as cancer therapeutics.

We provide the first evidence that selectively blocking Axl kinase function with an orally available small molecule has therapeutic value in inhibiting carcinoma tumor metastasis

in vivo. In contrast to diminished subcutaneous tumor growth generated by Axl knockdown (6), R428 did not affect growth of orthotopically implanted 4T1 tumors. This perhaps reflects a specific requirement for Axl to facilitate growth and colonization in foreign microenvironments. R428 significantly reduced metastasis in the MDA-MB-231-luc-D3H2LN model, which reflects tumor cell extravasation and colonization and excludes invasion and intravasation steps, and

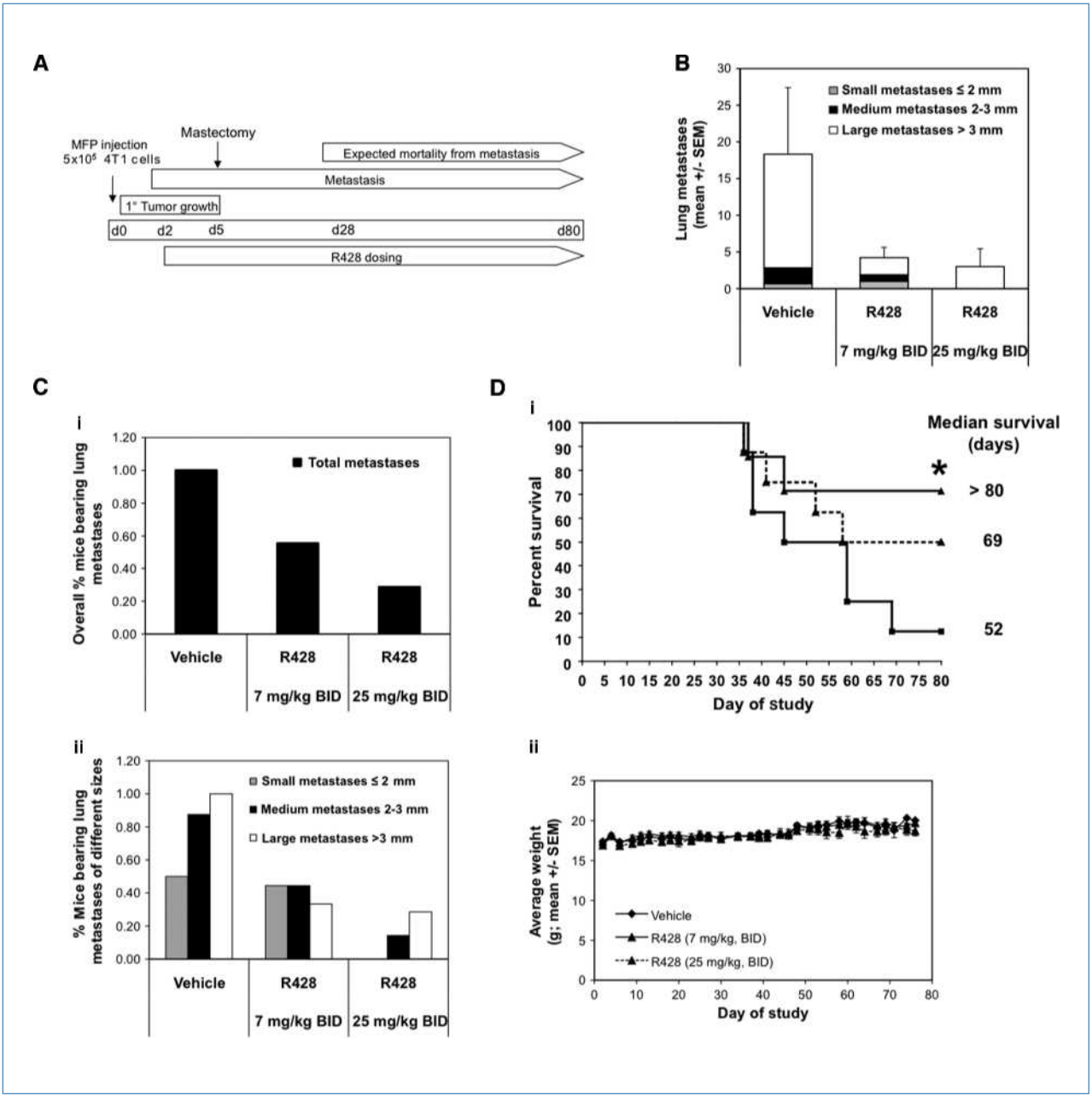

Figure 5. A, experimental protocol for 4T1 mastectomy survival study. Female BALB/c mice were injected in the mammary fat pad with 5×10^5 4T1 cells. A mastectomy was performed on day 5. Treatment with vehicle or R428 [7 and 25 mg/kg twice daily (BID)] was initiated on day 2 and continued until termination on day 80. B, R428 treatment reduces 4T1 lung metastasis. Lung metastases were counted on individual cull days and categorized as small (≤2 mm; gray fill), medium (2–3 mm; black fill), and large (≥3 mm; white fill). Two vehicle animals had too many large lung metastases to count individually and were scored as 50 large metastases each. SEMs are for mean total metastases. C, R428 reduces % of mice bearing macroscopic lung metastases. Overall incidence (i) and incidence (ii) of small (≤2 mm; gray fill), medium (2–3 mm; black fill), and large (≥3 mm; white fill) lung metastases. D, R428 prolongs survival of mice implanted with 4T1 tumors. i, Kaplan-Meier plot of % survival in vehicle (–■–) and R428 at 7 (–▲–) and 25 (–▲–) mg/kg twice daily groups. Mice that died before day 28 or developed primary tumor regrowth were excluded from analysis. *, $P < 0.05$ versus vehicle control, log-rank test. ii, mean body weight of animals on study.

bone marrow–derived cell (BMDC) recruitment by primary tumor–derived cytokines. R428, therefore, blocks processes associated with later stages of metastasis development (i.e., extravasation, organ seeding, and/or colonization and growth in microniches). However, we were not able to distinguish specifically which processes R428 inhibits *in vivo* from this study.

4T1 cells are aggressively metastatic. Characteristic large 4T1 lung metastases develop rapidly and intravascularly and only invade the surrounding tissue when they outgrow the capillary (26, 38). Conversely, the liver is colonized later by single tumor cells (39), which initially form micrometastases in the liver parenchyma. 4T1 cell metastasis was very sensitive to Axl blockade; R428 (7–25 mg/kg twice daily) was sufficient to block tumor cell dissemination. R428 reduced overall lung metastases by >50% in both 4T1 protocols and potently blocked development of liver micrometastases. R428 suppressed Snail expression *in vivo*. Thus, EMT reversal may be one mechanism by which R428 blocks metastasis. R428 also seemed to suppress metastasis growth. Inhibition of neovascularization and 4T1 cell survival by R428 are likely contributing factors. R428 reduced both tumor-expressed inflammatory cytokines and the corresponding host leukemoid response. Together, these data suggest that R428 may prevent metastasis seeding, colonization (survival of nascent micrometastases), and growth. Our data support potential mechanisms, including inhibition of cancer cell EMT, invasion, survival, growth in a foreign microenvironment, and cytokine secretion, as well host responses, including angiogenesis and mobilization of BMDCs.

The ultimate test of efficacy of cancer drugs is prolonged survival. R428 treatment clearly reduced metastasis-related mortality of 4T1-implanted mice. Moreover, in the MDA-MB-231 model, R428 treatment generated a similar survival extension to paclitaxel. Animals treated with 25 mg/kg R428 developed fewer 4T1 lung metastases than those treated with 7 mg/kg R428 in this study. Median survival, however, was longer in animals treated with the lower dose of R428. Undetected compound toxicity over the >11-week course of the study could potentially explain this discrepancy. Alternatively, as no significant difference was noted between survival of the two R428-treated groups, this difference may reflect inherent variability of the model.

As an antimetastatic therapy, R428 would likely be combined with the standard-of-care cytotoxic/antiproliferative agent in an adjuvant setting. It is therefore noteworthy that R428 enhanced the efficacy of a suboptimal dose of cisplatin *in vivo*. Moreover, in light of recent data suggesting that VEGF and VEGFR2 blockers ultimately increase tumor invasiveness (40–42), it may be necessary to combine these inhibitors with compounds that specifically block tumor-invasive processes, such as R428.

In this study, we focus on Axl function in breast cancer. Axl is highly expressed in invasive breast cancer cells and Axl knockdown blocks the invasive phenotype. Moreover, high Axl expression in primary breast tumors is a strong independent predictor of poor patient outcome (16). R428 clearly inhibits metastasis, the primary cause of breast cancer patient mortality, and prolongs survival in *in vivo* models of breast cancer metastasis. Axl also regulates invasiveness in GBM, lung, esophageal, pancreatic, and gastric carcinomas (7–10).[3] It will be important to determine the efficacy of R428 against metastasis/invasive spread of these and other cancer types. The data presented here offer persuasive evidence for the clinical development of Axl inhibitors as antimetastatic agents in breast cancer and potentially other solid tumors.

Disclosure of Potential Conflicts of Interest

All authors, except J. Chua and R. Brandt, are employees of Rigel, Inc.

Acknowledgments

We thank Emily Stauffer, Joanne Litvak, Rachel Mandell, Caroline Sula, and Jorge Victorino for technical assistance; Patrick McConnville and Vinod Kaimal for conducting the MDA-MB-231-luc-D3H2LN model; and Sheri Routt for performing the corneal micropocket model.

The costs of publication of this article were defrayed in part by the payment of page charges. This article must therefore be hereby marked *advertisement* in accordance with 18 U.S.C. Section 1734 solely to indicate this fact.

Received 8/13/09; revised 10/29/09; accepted 11/18/09; published OnlineFirst 2/9/10.

References

1. O'Bryan JP, Frye RA, Cogswell PC, et al. axl, a transforming gene isolated from primary human myeloid leukemia cells, encodes a novel receptor tyrosine kinase. Mol Cell Biol 1991;11:5016–31.
2. Janssen JW, Schulz AS, Steenvoorden AC, et al. A novel putative tyrosine kinase receptor with oncogenic potential. Oncogene 1991;6:2113–20.
3. Hafizi S, Dahlback B. Signalling and functional diversity within the Axl subfamily of receptor tyrosine kinases. Cytokine Growth Factor Rev 2006;17:295–304.
4. Linger RM, Keating AK, Earp HS, Graham DK. TAM receptor tyrosine kinases: biologic functions, signaling, and potential therapeutic targeting in human cancer. Adv Cancer Res 2008;100:35–83.
5. Bose R, Molina H, Patterson AS, et al. Phosphoproteomic analysis of Her2/neu signaling and inhibition. Proc Natl Acad Sci U S A 2006;103:9773–8.
6. Holland SJ, Powell MJ, Franci C, et al. Multiple roles for the receptor tyrosine kinase axl in tumor formation. Cancer Res 2005;65:9294–303.
7. Vajkoczy P, Knyazev P, Kunkel A, et al. Dominant-negative inhibition of the Axl receptor tyrosine kinase suppresses brain tumor cell growth and invasion and prolongs survival. Proc Natl Acad Sci U S A 2006;103:5799–804.
8. Koorstra JB, Karikari CA, Feldmann G, et al. The Axl receptor tyrosine kinase confers an adverse prognostic influence in pancreatic cancer and represents a new therapeutic target. Cancer Biol Ther 2009;8:618–26.
9. Sawabu T, Seno H, Kawashima T, et al. Growth arrest-specific gene 6 and Axl signaling enhances gastric cancer cell survival via Akt pathway. Mol Carcinog 2007;46:155–64.
10. Shieh YS, Lai CY, Kao YR, et al. Expression of axl in lung adenocarcinoma and correlation with tumor progression. Neoplasia 2005;7:1058–64.

11. Tai KY, Shieh YS, Lee CS, Shiah SG, Wu CW. Axl promotes cell invasion by inducing MMP-9 activity through activation of NF-κB and Brg-1. Oncogene 2008;27:4044–55.
12. Zhang YX, Knyazev PG, Cheburkin YV, et al. AXL is a potential target for therapeutic intervention in breast cancer progression. Cancer Res 2008;68:1905–15.
13. Hutterer M, Knyazev P, Abate A, et al. Axl and growth arrest-specific gene 6 are frequently overexpressed in human gliomas and predict poor prognosis in patients with glioblastoma multiforme. Clin Cancer Res 2008;14:130–8.
14. Rochlitz C, Lohri A, Bacchi M, et al. Axl expression is associated with adverse prognosis and with expression of Bcl-2 and CD34 in *de novo* acute myeloid leukemia (AML): results from a multicenter trial of the Swiss Group for Clinical Cancer Research (SAKK). Leukemia 1999;13:1352–8.
15. Gustafsson A, Martuszewska D, Johansson M, et al. Differential expression of Axl and Gas6 in renal cell carcinoma reflecting tumor advancement and survival. Clin Cancer Res 2009;15:4742–9.
16. Gjerdrum C, Tiron C, Høiby T, et al. Axl is an essential epithelial-to-mesenchymal transition-induced regulator of breast cancer metastasis and patient survival. Proc Natl Acad Sci U S A. Epub 2010 Jan 4.
17. Elvin P, Garner AP. Tumour invasion and metastasis: challenges facing drug discovery. Curr Opin Pharmacol 2005;5:374–81.
18. Jenkins DE, Hornig YS, Oei Y, Dusich J, Purchio T. Bioluminescent human breast cancer cell lines that permit rapid and sensitive *in vivo* detection of mammary tumors and multiple metastases in immune deficient mice. Breast Cancer Res 2005;7:R444–54.
19. Goff D, Zhang J, Singh R, et al. Inventors, Rigel Pharmaceuticals, Inc., assignee. Polycyclic heteroaryl substituted triazoles useful as Axl inhibitors. United States patent 20080188455. 2008 Aug 7.
20. Braselmann S, Taylor V, Zhao H, et al. R406, an orally available spleen tyrosine kinase inhibitor blocks fc receptor signaling and reduces immune complex-mediated inflammation. J Pharmacol Exp Ther 2006;319:998–1008.
21. Brenes F, Harris S, Paz MO, Petrovic LM, Scheuer PJ. PLP fixation for combined routine histology and immunocytochemistry of liver biopsies. J Clin Pathol 1986;39:459–63.
22. Hanfelt JJ. Statistical approaches to experimental design and data analysis of *in vivo* studies. Breast Cancer Res Treat 1997;46:279–302.
23. Braunger J, Schleithoff L, Schulz AS, et al. Intracellular signaling of the Ufo/Axl receptor tyrosine kinase is mediated mainly by a multi-substrate docking-site. Oncogene 1997;14:2619–31.
24. Mahadevan D, Cooke L, Riley C, et al. A novel tyrosine kinase switch is a mechanism of imatinib resistance in gastrointestinal stromal tumors. Oncogene 2007;26:3909–19.
25. Schroeder GM, An Y, Cai ZW, et al. Discovery of *N*-(4-(2-amino-3-chloropyridin-4-yloxy)-3-fluorophenyl)-4-ethoxy-1-(4-fluorophenyl)-2-oxo-1,2-dihydropyridine-3-carboxamide (BMS-777607), a selective and orally efficacious inhibitor of the Met kinase superfamily. J Med Chem 2009;52:1251–4.
26. Aslakson CJ, Miller FR. Selective events in the metastatic process defined by analysis of the sequential dissemination of subpopulations of a mouse mammary tumor. Cancer Res 1992;52:1399–405.
27. DuPre SA, Hunter KW, Jr. Murine mammary carcinoma 4T1 induces a leukemoid reaction with splenomegaly: association with tumor-derived growth factors. Exp Mol Pathol 2007;82:12–24.
28. DuPre SA, Redelman D, Hunter KW, Jr. The mouse mammary carcinoma 4T1: characterization of the cellular landscape of primary tumours and metastatic tumour foci. Int J Exp Pathol 2007;88:351–60.
29. Pande K, Ueda R, Machemer T, et al. Cancer-induced expansion and activation of $CD11b^+$ $Gr\text{-}1^+$ cells predispose mice to adenoviral-triggered anaphylactoid-type reactions. Mol Ther 2009;17:508–15.
30. Wang Z, Spaulding B, Sienko A, et al. Mammaglobin, a valuable diagnostic marker for metastatic breast carcinoma. Int J Clin Exp Pathol 2009;2:384–9.
31. Nofech-Mozes S, Holloway C, Hanna W. The role of cytokeratin 5/6 as an adjunct diagnostic tool in breast core needle biopsies. Int J Surg Pathol 2008;16:399–406.
32. Polyak K, Weinberg RA. Transitions between epithelial and mesenchymal states: acquisition of malignant and stem cell traits. Nat Rev Cancer 2009;9:265–73.
33. Giamas G, Stebbing J, Vorgias CE, Knippschild U. Protein kinases as targets for cancer treatment. Pharmacogenomics 2007;8:1005–16.
34. Lay JD, Hong CC, Huang JS, et al. Sulfasalazine suppresses drug resistance and invasiveness of lung adenocarcinoma cells expressing AXL. Cancer Res 2007;67:3878–87.
35. Hong CC, Lay JD, Huang JS, et al. Receptor tyrosine kinase AXL is induced by chemotherapy drugs and overexpression of AXL confers drug resistance in acute myeloid leukemia. Cancer Lett 2008;268:314–24.
36. Liu L, Greger J, Shi H, et al. Novel mechanism of lapatinib resistance in HER2-positive breast tumor cells: activation of AXL. Cancer Res 2009;69:6871–8.
37. D'Arcangelo D, Gaetano C, Capogrossi MC. Acidification prevents endothelial cell apoptosis by Axl activation. Circ Res 2002;91:e4–12.
38. Wong CW, Song C, Grimes MM, et al. Intravascular location of breast cancer cells after spontaneous metastasis to the lung. Am J Pathol 2002;161:749–53.
39. Luzzi KJ, MacDonald IC, Schmidt EE, et al. Multistep nature of metastatic inefficiency: dormancy of solitary cells after successful extravasation and limited survival of early micrometastases. Am J Pathol 1998;153:865–73.
40. Ebos JM, Lee CR, Cruz-Munoz W, Bjarnason GA, Christensen JG, Kerbel RS. Accelerated metastasis after short-term treatment with a potent inhibitor of tumor angiogenesis. Cancer Cell 2009;15:232–9.
41. Loges S, Mazzone M, Hohensinner P, Carmeliet P. Silencing or fueling metastasis with VEGF inhibitors: antiangiogenesis revisited. Cancer Cell 2009;15:167–70.
42. Paez-Ribes M, Allen E, Hudock J, et al. Antiangiogenic therapy elicits malignant progression of tumors to increased local invasion and distant metastasis. Cancer Cell 2009;15:220–31.